'89 韓國自動制御學術會議論文集 1989. 10. 27~28

# SUBOPTIMAL VIBRATION CONTROL OF FLEXIBLE ROTOR BEARING SYSTEM BY USING A MAGNETIC BEARING

Chong-Won Lee* and Jong-Sun Kim**

* Department of Mechanical Engineering, Korea Advanced Institute of Science and Technology

** Department of Mechanical and Precision Engineering, Kumoh Institute of Technology

A suboptimal output feedback controller is designed and applied to a flexible rotor bearing system in order to control the unstable or lightly damped vibrations. The reduced order model is the truncated modal equation of the distributed parameter system obtained through the singular perturbation. The instability problem arising from the spillover effects caused by the uncontrolled high frequency modes is prevented through the constrained optimization by incorporating the spillover term into the performance index. The efficiency of the proposed method is demonstrated experimentally with a flexible rotor by using a magnetic bearing.

## 1. INTRODUCTION

The vibration induced by sudden imbalance or external loading may cause large amplitude displacements relative to the support structure, large shock loads at the intershaft and support structure, and/or large internal forces in the rotating assemblies. In recent years, advanced development of electromagnetic bearing technology enables the active control of rotor bearing systems to be in practical use with relatively low cost and high reliability[1], hence further improvement in vibration reduction may be achieved by using active control techniques. Gondhalekar et al.[2] investigated an electromagnetic damper as applied to a transmission shaft passing through a critical speed. Anton and Ulbrich[3] performed an output feedback control using a magnetic bearing in asymmetrical rotor bearing system. Salm and Schweitzer[4] discussed spillover effects resulting from the control of a flexible rotor bearing system based on the reduced order model in output feedback. Bradfield et al.[5] studied the digital control of supercritical shaft by using electromagnetic bearing.

However, most of the previous works essentially have not accounted for the distributed parameter nature of flexible rotor bearing systems, even though it is sure important to design a finite dimensional feedback controller for on-line implementation[6]. In this paper, the digital implementation of the constrained output feedback controller developed in the previous work[7] is experimentally studied using an electromagnetic bearing and related control circuits developed in the laboratory. The control scheme primarily emphasizes the stabilization against observation/control spillover effects through constrained optimization.

## 2. THEORETICAL DEVELOPMENT

### 1) Modeling

The equations of motion and of observation for a flexible rotor bearing system can be written as[8]

$$\mathbf{M}_q(x)\ddot{\mathbf{q}}(x,t) + \mathbf{C}_q(x)\dot{\mathbf{q}}(x,t) + \mathbf{K}_q(x)\mathbf{q}(x,t) = \Gamma(x)\mathbf{u}(t)$$

$$\mathbf{y}(t) = \Upsilon_q(x)\mathbf{q}(x,t) + \Upsilon_{\dot{q}}(x)\dot{\mathbf{q}}(x,t) \qquad (1)$$

where $\mathbf{M}_q$, $\mathbf{C}_q$ and $\mathbf{K}_q$, mainly consisting of partial differential operators and symbolic functions, represent the mass, damping and stiffness operators, respectively. Each operators are neither symmetric nor positive definite due to the gyroscopic effect, internal/external damping terms and asymmetric bearing property. $\Upsilon_q$, $\Upsilon_{\dot{q}}$ and $\Gamma$ are the displacement sensor, velocity sensor and actuator influence operators, respectively. The influence functions usually consist of almost Dirac delta functions since the control devices are localized, e.g. point sensors and point actuators, in practice. The vector $\mathbf{q}(x,t) = [y(x,t) \quad z(x,t)]^t$ is the associated distributed displacement vector along the shaft, $\mathbf{y} \in R^r$ the output vector, and $\mathbf{u} \in R^m$ the input vector. The displacement $\mathbf{q}$ is subject to given initial and boundary conditions. Introducing the state $\mathbf{p} = [\dot{\mathbf{q}}^t \quad \mathbf{q}^t]^t$, Eq. (1) can be written, in the state space form, as

$$\mathbf{E}(x)\dot{\mathbf{p}}(x,t) = \mathbf{A}(x)\mathbf{p}(x,t) + \mathbf{B}(x)\mathbf{u}(t) \qquad (2a)$$

$$\mathbf{y}(t) = \mathbf{C}(x)\mathbf{p}(x,t) \qquad (2b)$$

where

$$\mathbf{E} = \begin{bmatrix} 0 & \mathbf{M}_q \\ \mathbf{M}_q & \mathbf{C}_q \end{bmatrix}, \quad \mathbf{A} = \begin{bmatrix} \mathbf{M}_q & 0 \\ 0 & -\mathbf{K}_q \end{bmatrix}, \quad \mathbf{B} = \begin{bmatrix} 0 \\ \Gamma \end{bmatrix}, \quad \mathbf{C} = [\Upsilon_{\dot{q}} \quad \Upsilon_q]$$

By means of the modal transformation $\phi(\cdot) = [\langle \psi_1, \cdot \rangle \ \langle \psi_2, \cdot \rangle \ \langle \psi_2, \cdot \rangle \ \cdots\cdots]^t$ and the modal expansion $\mathbf{p}(x,t) = \sum_{i=1}^{\infty} \varphi_i(x)\zeta_i(t)$, a set of modal equations can be obtained as

$$\dot{\zeta}(t) = \mathbf{A}_m\zeta(t) + \mathbf{B}_m\mathbf{u}(t) \qquad (3a)$$

$$\mathbf{y}(t) = \mathbf{C}_m\zeta(t) \qquad (3b)$$

where

$$A_m = \Phi(A\Phi),\ B_m = \Phi(B),\ C_m = C\Phi$$
$$\Phi = [\varphi_1\ \ \varphi_2\ \ \varphi_3\ \cdots\cdots]$$

and $\zeta = [\zeta_1\ \ \zeta_2\ \ \zeta_3\ \cdots\cdots]^t$ is the complex modal state vector. The eigenfunction $\varphi_i$ and the adjoint $\psi_i$ satisfy the biorthonormality relation

$$<\psi_i, E\varphi_j> = \delta_{ij} \text{ and } <\psi_i, A\varphi_j> = \lambda_i\delta_{ij} \qquad (4)$$

Dividing the modal state into three classes, primary, secondary and residual modes, Eq. (3) can be rewritten, neglecting the residual modes, as

$$\dot{\zeta}_p(t) = A_p\zeta_p(t) + B_p u(t) \qquad (5a)$$
$$\dot{\zeta}_s(t) = A_s\zeta_s(t) + B_s u(t) \qquad (5b)$$
$$y(t) = C_p\zeta_p(t) + C_s\zeta_s(t) \qquad (5c)$$

where the $n_p$–dimensional primary modal state vector $\zeta_p$ is made up of the states of significance, forming a modal subspace. The secondary modal state $\zeta_s$ consists of the modes of significance in stability but insignificance in control performance. In rotor–bearing systems, especially in overhung type rotors or rigid rotors with relatively soft bearings, the primary and secondary modes are relatively well separated so that the two–time scale assumption might be well justified. By applying the singular perturbation to the secondary modes, further model reduction can be achieved so as to give

$$\dot{\zeta}_0(t) = A_0\zeta_0(t) + B_0 u(t) \qquad (6a)$$
$$y(t) = C_0\zeta_0(t) + D_0 u(t) \qquad (6b)$$

where $A_0 = A_p$, $B_0 = B_p$, $C_0 = C_p$ and $D_0 = -C_s A_s^{-1} B_s$. The direct term $D_0 u$ in the reduced order model is equivalent to the residual flexibility.

2) Constrained Output Feedback Control

Consider an optimal dynamic compensator of the form

$$\dot{z}(t) = A_z z(t) + B_z y(t) \qquad (7a)$$
$$u(t) = C_z z(t) + D_z y(t) \qquad (7b)$$

with the performance index

$$J = \int_0^\infty (\zeta_0^t Q_0 \zeta_0 + z^t Q_1 z + u^t R_0 u + \dot{z}^t R_1 \dot{z})dt \qquad (8)$$

where $z \in R^{n_z}$ is the compensator state vector, and $Q_0$ and $Q_1$ are to be positive semi–definite, and $R_0$ and $R_1$ to be positive definite. Augmenting the state of the system with the compensator equation, one obtains

$$\dot{\hat{\zeta}}(t) = \hat{A}_c\hat{\zeta}(t) \qquad (9)$$

where

$$\hat{\zeta}(t) = [\zeta_0^t(t)\ \ z^t(t)]^t$$
$$\hat{A}_c = \hat{A} + \hat{B}\hat{K}\hat{C}$$

$$\hat{A} = \begin{bmatrix} A_0 & 0 \\ 0 & 0 \end{bmatrix},\ \hat{B} = \begin{bmatrix} B_0 & 0 \\ 0 & I \end{bmatrix},\ \hat{C} = \begin{bmatrix} C_0 & 0 \\ 0 & I \end{bmatrix},\ \hat{K} = \begin{bmatrix} \hat{D}_z & \hat{C}_z \\ \hat{B}_z & \hat{A}_z \end{bmatrix}$$

and

$$\hat{D}_z = (I - D_z D_0)^{-1} D_z,\ \hat{C}_z = (I - D_z D_0)^{-1} C_z$$
$$\hat{B}_z = B_z(I - D_0 D_z)^{-1},\ \hat{A}_z = A_z + \hat{B}_z D_0 C_z$$

It is well known that the closed loop poles approximately consist of the eigenvalues $\lambda[\hat{A}_c]$ and $\lambda[A_s + B_s D_z C_s]$[9]. Even if Re $\lambda[\hat{A}_c] < 0$ by design and Re $\lambda[A_s] \le 0$, it does not necessarily lead to the stability condition for the secondary modes

$$\text{Re } \lambda[A_s + B_s D_z C_s] \le 0 \qquad (10)$$

The main idea is that, if the observation and/or control spillovers are unavoidable, that is $B_s \neq 0$ and $C_s \neq 0$, since the actuators or sensors cannot be located exactly on the nodes of all secondary modes, the spillover effects should be accounted for, if possible, so as to stabilize the secondary system.

The constrained output feedback control offers a remedy to the spillover problem by minimizing the modified performance index, using the trace identity, as

$$J_a = \text{tr}[PW_0] + \text{tr}[F^t\mathcal{R}(\hat{K}, P)] + \text{tr}[S(A_s + B_s D_z C_s)] + \text{tr}[T\{D_z - \hat{D}_z(I + D_0\hat{D}_z)^{-1}\}] \qquad (11)$$

where

$$W_0 = \begin{bmatrix} E\{\zeta_0(0)\zeta_0^t(0)\} & 0 \\ 0 & E\{z(0)z^t(0)\} \end{bmatrix}$$

and P satisfies the matrix Riccati equation

$$(\hat{A}+\hat{B}\hat{K}\hat{C})^t P + P(\hat{A}+\hat{B}\hat{K}\hat{C}) + \hat{Q} + \hat{C}^t\hat{K}^t\hat{R}\hat{K}\hat{C} = 0$$
$$= \mathcal{R}(\hat{K}, P) \qquad (12)$$
$$\hat{Q} = \begin{bmatrix} Q_0 & 0 \\ 0 & Q_1 \end{bmatrix},\ \hat{R} = \begin{bmatrix} R_0 & 0 \\ 0 & R_1 \end{bmatrix}$$

and $S = \text{Diag}(s_1, s_2, \cdots\cdots, s_{n_s})$ is the positive definite weighting matrix to the spillover term. Each element of S represents the weighting for the corresponding mode and F and T are the Lagrange multiplier matrices of appropriate dimensions. $E$ denotes the expectation. The necessary conditions, using the matrix minimum principle, are obtained from

$$\frac{\partial J_a}{\partial F} = \frac{\partial J_a}{\partial P} = \frac{\partial J_a}{\partial \hat{K}} = \frac{\partial J_a}{\partial T} = \frac{\partial J_a}{\partial K} = 0 \qquad (13)$$

The above equations can be expanded to give

$$(\hat{A} + \hat{B}\hat{K}\hat{C})^t P + P(\hat{A} + \hat{B}\hat{K}\hat{C}) + \hat{Q} + \hat{C}^t\hat{K}^t\hat{R}\hat{K}\hat{C} = 0$$
$$(\hat{A} + \hat{B}\hat{K}\hat{C})F + F(\hat{A} + \hat{B}\hat{K}\hat{C})^t + W_0 = 0$$
$$\hat{K} = -\hat{R}^{-1}[\hat{B}^t P F\hat{C}^t - I_m(I - D_z D_0)^t T^t I_r^t](\hat{C}F\hat{C}^t)^{-1}$$
$$D_z = \hat{D}_z(I + D_0\hat{D}_z)^{-1}$$
$$T = -(I + D_0 D_z)^{-1} C_s S B_s$$

where

$$K = \begin{bmatrix} D_z & C_z \\ B_z & A_z \end{bmatrix}, \quad I_m = \begin{bmatrix} I_{m\times m} \\ 0_{s\times m} \end{bmatrix}, \quad I_r = \begin{bmatrix} I_{r\times r} \\ 0_{s\times r} \end{bmatrix}$$

## 3. EXPERIMENT

1) Experimental Set–up

Figure 1 shows the schematic of experimental setup. The flexible shaft, 680 mm long and 30 mm in diameter, assembled with four rigid disks is supported by two self–aligning type of radial ball bearings. A magnetic bearing as a force actuator is located at the free end of the overhung rotor, which is activated by the current supplied from the power amplifier. The magnetic bearing has four identical radial electromagnets equally spaced around a 160 mm diameter magnetic disk. The core material is made of laminated stacks of silicon steel to reduce the eddy current effect. Linearizing the magnetic force w.r.t. the neutral position, the net magnetic force f due to small perturbation $i_c$ in control current can be expressed by

$$f(t) = k_i i_c(t)$$

where the current stiffness $k_i$ implies the sensitivity of magnetic force relative to the control current $i_c$. The identified value is 14.12 N/V in the vertical direction and 14.98 N/V in the horizontal direction when the steady state current is 0.5 A and the total airgap is 1.5 mm.

A pair of eddy current type proximity probes located at 0.191 m apart from the driven end as shown in Fig. 1 measure the vertical (Y) and horizontal (Z) displacements of the geometric center of the shaft. In order to directly measure the control force exerted on the rotor, a three axes tool dynamometer is placed between the mount fixture and the magnetic bearing. In order to surmount the difficulties with high frequency noise contamination generated during operation, two low pass filters with cutoff frequency of 400 Hz are used.

The controller is a hybrid system consisting of analog circuits and a digital computer. The power amplifiers and compensation networks constitute the analog components which supply the control current to the magnets and ensure the linear conversion between the control signal and the generated control force. A 16–bit personal computer (IBM–PC AT) equipped with 12–bit data translation device is the main part for the digital control implementation, which controls the peripheral devices and it also calculates the control input based on the measured sensor output.

2) System Identification

A sequence of Gaussian random data is D/A converted, and transformed to current through the power amplifiers, driving the magnet and exciting the rotor system. At the same time the measured magnetic force and displacement response signals are low pass filtered with cutoff frequency of 400 Hz, A/D converted and then stored on the memory for further processing. Throughout the experiments, the sampling rate is kept to be 400 Hz. The experiments are repeated at several operating speeds.

The modal parameters are extracted by multimode curve fitting of the measured frequency response functions. The results are summarized in Table 1. As the operating speed increases, it can be said that the completely coupled modes of the rotor at rest are separated into the forward and backward modes as the gyroscopic moment tends to stiffen the forward modes and soften the backward modes. The gyroscopic effect makes the system to be controlled by a uni–directional actuator, not a bi–directional one, since the uni–directional excitation causes the vibration perpendicular to the excitation direction.

3) Control Experiments and Discussions

Using the identified modal parameters at 3000 rpm, the output feedback controllers are designed by minimizing the quadratic penalty index (11) with

$$Q_0 = 1000I \qquad R_0 = I \qquad S = sI$$

where the first forward and backward mode pair are chosen as the primary modes and the second mode pair as the secondary modes. The control objective is to suppress the vibration of the primary modes while maintaining the secondary modes to be stable. As shown in Table 2, the unconstrained feedback controller makes the closed loop system unstable since one of the secondary modes (forward mode) has negative damping. Hence it is required to make the secondary modes stable by constrained optimization. As the parameter s increases, the second modes become stable while the primary modes become less stable. As shown in Table 2, the controller with $s = 0.4$ is found to be satisfactory for the dual objectives, performance and stability.

To show the performance of the proposed controller, the constrained($S = 0.4I$) and unconstrained($S = 0$) controllers are designed. To implement the controller in a digital computer, the continuous time controller is discretized with the 1 kHz sampling rate.

Figure 2 shows the impulse response of the uncontrolled system when the rotor displacement is measured at the sensor location when the computer generated impulsive force with magnitude of 70 N and duration of 0.01 sec. is applied at the actuator position in the vertical direction. The results are compared with the simulation results obtained numerically based on the experimentally determined model. The damping ratio of the open loop system is so small (about 0.008) that the transient vibration tends to sustain for a long period of time. Figure 3 shows the impulse response, along with the simulation results, when the constrained output feedback control acts. The increase in damping due to control is notable. From the response in Fig. 3, the damping ratios of the first mode pair are found to be approximately 0.04, somewhat smaller than the designed values of 0.05 as already shown in Table 2. Figure 4 shows the impulse response when the unconstrained output feedback control acts. Notice that in the unconstrained control system the second mode becomes unstable due to the spillover effects.

## 4. CONCLUDING REMARKS

The magnetic bearing of four magnets type is manufactured in order to apply the non–contacting control force to the rotor system during operation. Preliminary tests are preceded in order to check the reliable operation and to identify the parameters necessary to the controller design. Measurements of the vibrational response subject to the impulse disturbance confirm the numerical results with fair accuracy. From

the experimental results, it can be concluded that the proposed controller can be used effectively in improving the performances of lightly damped rotor systems, while preserving stability against spillover effects.

## REFERENCES


1. Habermann, H., and G. Liard, "An active magnetic bearing system," *Tribology International*, **13**, 85–89, 1980.

2. Gondhalekar, V. M., J. Nikolajsen, and B. V. Jayawant, "Electromagnetic control of flexible transmission shaft vibrations," *Proc. IEE*, **126**, 1008–1010, 1979.

3. Anton, E., and H. Ulbrich, "Active control of vibrations in the case of asymmetrical high–speed rotors by using magnetic bearings," *ASME J. of Vibration, Acoustics, Stress, and Reliability in Design*, **107**, 410–415, 1985.

4. Salm, J., and G. Schweitzer, "Modeling and control of a flexible rotor with magnetic bearings," *3rd Int. Conf. on Vibrations in Rotating Machinery*, C277/84, 553–561, 1984.

5. Bradfield, C. D., J. B. Roberts, and R. Karunendiran, "Performance of an electromagnetic bearing for the vibration control of a supercritical shaft," *Proc. Instn of Mechanical Engineers*, **201**, 201–212, 1987.

6. Balas, M. J., "Active control of flexible systems," *J. of Optimization Theory and Applications*, 25, 415–436, 1978.

7. Kim, J. S., and C. W. Lee, "Constrained output feedback control of flexible rotor bearing systems," to appear in *J. of Sound and Vibration*.

8. Kim, J. S., Optimum vibration control of distributed parameter rotor bearing systems by using electromagnetic bearing, *Ph. D dissertation*, 1989.

9. O'Reilly, J., "Robustness of linear feedback control systems to unmodelled high–frequency dynamics," *Int. J. Control*, **44**, 1077–1088, 1986.


TABLE 1 Identified Modal Parameters
(F=Forward Mode, B=Backward Mode)

| Spin speed Ω (rpm) | Mode | Identified: Natural frequency (Hz) | Identified: Damping ratio |
|---|---|---|---|
| 0 | 1F | 61.650 | 0.00836 |
| | 1B | 61.494 | 0.00931 |
| | 2F | 135.020 | 0.03470 |
| | 2B | 135.030 | 0.03220 |
| 3000 | 1F | 62.945 | 0.00790 |
| | 1B | 59.175 | 0.00807 |
| | 2F | 136.450 | 0.03094 |
| | 2B | 132.840 | 0.03764 |

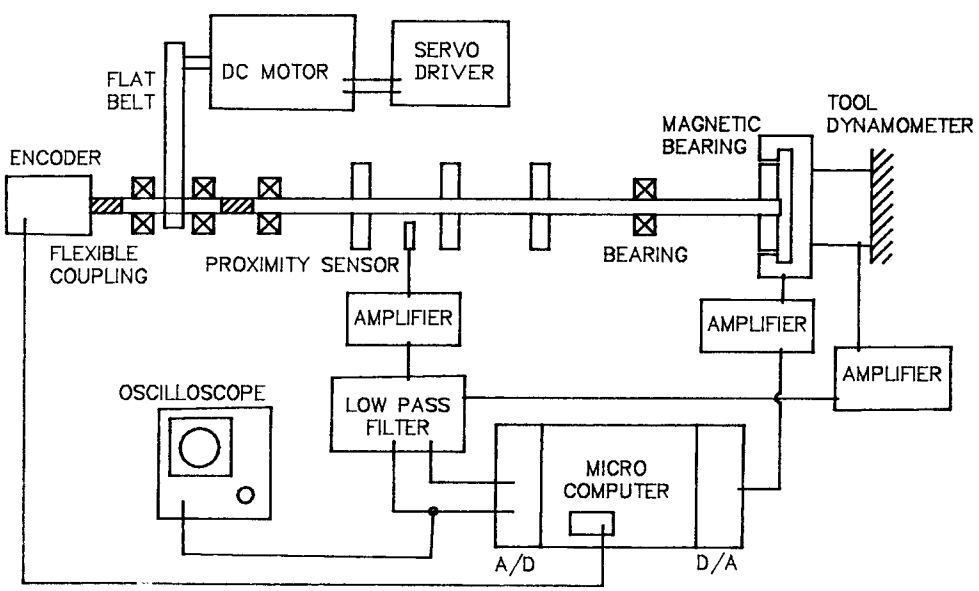


Fig. 1 Schematic of experimental set–up.

TABLE 2 Open Loop and Closed Loop Eigenvalues
(F=Forward Mode, B=Backward Mode)

| Mode | Open Loop System | Closed Loop System | |
|---|---|---|---|
| N | | S = 0 | S = 0.4I |
| 1F | −3.124+j395.495 | −33.465+ j394.32 | −20.468+ j395.40 |
| 1B | −3.001−j371.808 | −31.604−j370.78 | −20.006−j371.71 |
| 2F | −26.526+j857.341 | 1.881+ j858.91 | −10.110+ j857.73 |
| 2B | −31.416−j834.658 | −4.304−j836.08 | −15.490−j835.04 |

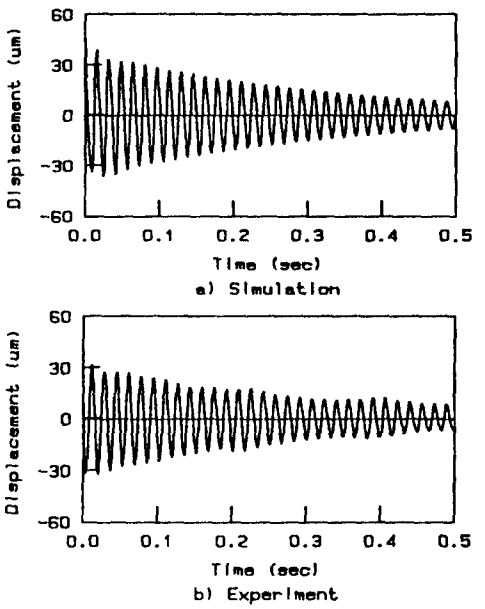


Fig. 2 Transient response of open loop system subject to Y–directional impulse force.

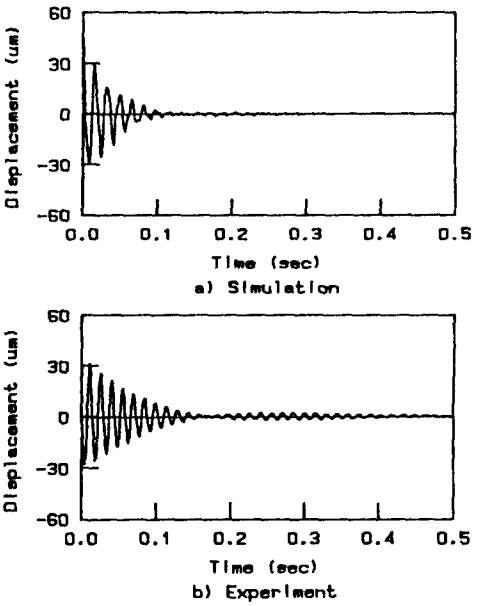


Fig. 3 Transient response of constrained control sytem subject to Y–directional impulse force.

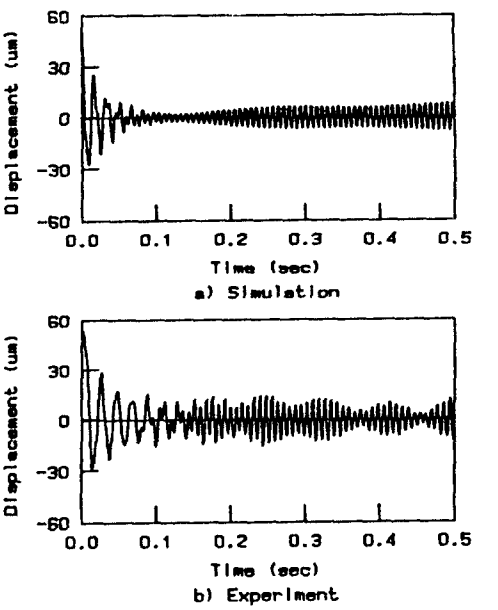


Fig. 4 Transient response of unconstrained control system subject to Y–directional impulse force.